

Development of an off-grid electrical vehicle charging station hybridized with renewables including battery cooling system and multiple energy storage units

Abdulla Al Wahedi, Yusuf Bicer

Item type

Journal Contribution

Terms of use

This work is licensed under a [CC BY 4.0](#) license

This version is available at

https://manara.qnl.qa/articles/journal_contribution/Development_of_an_off-grid_electrical_vehicle_charging_station_hybridized_with_renewables_including_battery_cooling_system_and_multiple_energy_s
Access the item on Manara for more information about usage details and recommended citation.

Posted on Manara – Qatar Research Repository on
2020-11-01



Research paper

Development of an off-grid electrical vehicle charging station hybridized with renewables including battery cooling system and multiple energy storage units

Abdulla Al Wahedi^{*}, Yusuf Bicer

Division of Sustainable Development (DSD), College of Science and Engineering (CSE), Hamad Bin Khalifa University (HBKU), Qatar Foundation (QF), Education City, Doha, Qatar

ARTICLE INFO

Article history:

Received 9 May 2020

Received in revised form 10 July 2020

Accepted 23 July 2020

Available online 3 August 2020

Keywords:

Stand-alone

Fast-charging

Solar energy

Biomass

Battery cooling

Fuel cells

ABSTRACT

Electric vehicles expansion is accelerating rapidly due to e-mobility's massive contribution in reducing fossil fuel consumption and CO₂ emissions. Fulfilling the charging requirements of millions of electrical vehicles from the grid would overload the network and introduce substantial burden on the power sector. This study proposes, and thermodynamically assesses, a grid-independent and renewable energy-based, stand-alone electrical vehicle charging station consisting of CPV/T, wind turbine and biomass combustion-based steam Rankine cycle plant. Hydrogen and ammonia-based fuel cells are integrated in the design along with electrochemical, chemical and thermal storage units to ensure uninterrupted charging services during night times and unfavorable weather conditions. Since the proposed design is suggested for use in the State of Qatar, which is located in a hot region, an absorption cooling system is incorporated to cool the produced NH₃ gas and convert it into liquid phase for optimal storage purposes and to maintain the operating temperature of the battery system within the allowable limits. The thermodynamic analysis followed in this study is based on writing the balance equations for mass, energy, entropy and exergy for the system's components along with their energy and exergy efficiency equations. The results show that the energy generated from renewable energy sources and fuel cells are sufficient to fast-charge 80 electrical vehicles daily. The energy efficiencies of H₂ fuel cell, NH₃ fuel cell, CPV/T, wind turbine and energetic COP of the absorption cooling system are found to be 77%, 72%, 45%, 43% and 0.72, respectively. The exergy efficiency of CPV/T and the exergetic COP of the absorption cooling system are found to be 37% and 0.19, respectively. The overall energy and exergy efficiencies of the proposed integrated system are found to be 45% and 19%, respectively.

© 2020 The Author(s). Published by Elsevier Ltd. This is an open access article under the CC BY license (<http://creativecommons.org/licenses/by/4.0/>).

1. Introduction

Power and transport sectors are considered two main dominant sources for consuming fossil fuel and emitting greenhouse gases (GHG) into the environment. Although e-mobility is considered as an eco-friendly solution to reduce the fossil fuel consumption and associated CO₂ emissions related to the transport sector, securing the required power through fossil-fuel based energy sources to charge the Electric Vehicles (EVs) will result in transferring the natural resources depletion and environmental pollution burdens from the transport sector to energy sector. The prevailing fossil fuel sources for electricity generation are natural gas and coal where approximately 0.5–0.97 kg of CO₂ is generated per kWh (Mittal, 2010). Since the current average

CO₂ concentration level in the atmosphere is 407.18 ppm and 350 ppm is the ideal value (Pro, 2017), the dependency on the conventional methods for generating the additional substantial electricity loads required to fulfill EVs charging demands will not only increase fossil fuel depletion rates but will also dramatically increase the negative environmental impacts due to the associated CO₂ emissions. Therefore, the integration of renewable energy sources (RES) with the electricity sector would be the optimal solution to preserve fossil fuels for future generations. It would also mitigate the hazardous emissions responsible for global warming and climate change.

On the other hand, e-mobility deployment expansions will lead to major technical challenges and severe negative impacts on the power grid, if the required substantial charging demand will be fulfilled through the electricity network. Both the transmission and distribution network and accompanying components of the electricity network will require major and costly upgrades. The experimental results conducted by Zou et al. (2020) to determine the impact of EV charging on the low voltage network

^{*} Corresponding author.

E-mail addresses: amalwahedi@hbku.edu.qa (A. Al Wahedi), ybicer@hbku.edu.qa (Y. Bicer).

showed negative effects on power quality due to overloading on transformers. Moreover, to safeguard the network, on-grid charging stations require scheduling EV charging behaviors, such as time and charging demand, upon arrival to a charging station; yet, these behaviors are uncertain and cannot be scheduled easily (Wang et al., 2020). The results in Girard et al. (2019) showed that EV charging does not achieve real environmental gains if charged through the grid while considerable reduction in CO₂ emissions per km traveled is achieved when using off-grid solar system for charging.

Therefore, deploying stand-alone distributed RES-based charging stations would be an optimal solution to boost EVs deployment globally in an eco-friendly manner with no impact on the existing power grid. However, stand-alone stations with RES usually are not capable of producing uninterrupted electrical power supply due to the intermittency and volatility of renewable sources. Because the variability of energy sources such as night times and cloudy weathers (in case of solar plants), wind speed fluctuations (in case of wind turbine plants) and availability of biomass feedstock (in case of biomass plants) are very critical (Suresh et al., 2019). To mitigate the intermittency issue, hybridization of multiple RES-based subsystems could be integrated to complement each other and achieve enhanced performance. To further improve the overall system's performance and reliability, alternative energy storage systems, such as electrochemical, chemical and thermal energy storage systems, could be incorporated as well.

Many studies and projects have employed solar photovoltaic (PV) and wind turbine technologies either individually or through hybridization to generate electricity which is used, or could be used, for charging EVs. Biyik and Kahraman (2019) presented a case study where a predictive controller to find the optimal solar system, battery storage, heating, ventilation and air conditioning (HVAC) system combination in multi-zone buildings is developed to minimize the peak load demand without compromising occupants' thermal comfort. The developed controller managed to reduce the average load by 23% compared to the baseline operation load. The same study has suggested to expand the research to include EV charging and wind turbine in future works; both are considered in this paper. In the study conducted by Mehrjerdi and Hemmati (2020), a demand response program is developed for a grid connected residential building equipped with local solar and wind systems to reduce energy cost and manage the intermittency nature of the incorporated RES. Interruptible, constant and uninterrupted load patterns were considered as various loads to be fulfilled on a daily basis. The optimization is based on dispatching and adjusting the loads to achieve maximum utilization of energy generated by RES and minimum cost of energy trade with the grid. The off-grid operation was discussed briefly in the same study which is investigated in depth in this paper. Mazzeo et al. (2020), a decision-making procedure is developed to assess the optimal solar, wind and battery subsystems portfolio and sizes that can be configured for specific loads to substitute the grid considering energy, economic and environmental aspects. EV charging was not investigated in that study and is considered in-depth in this current study. Mazzeo (2019) conducted an energy, economic and environmental based feasibility study in a residential area to select the optimal grid, solar and battery storage combination for a nocturnal EV charging. The generated energy from the solar system is used to fulfill the electrical load, charge the battery storage and forward the surplus energy to the grid. The study did not consider an off-grid scenario which is in fact one of the main objectives of this paper. Liu et al. (2015) investigated the smart grid integration with solar, wind and battery subsystems to achieve optimal EV charging based on cost, efficiency and

environmental aspects. The results showed that integrating RES into EV charging infrastructure assists in reducing the impact of EV demand expansion on the grid. The article raised two major technical concerns, which must be considered in future works. The first gap is the technical challenges due to integrating RES into the network and microgrid systems. The second gap is the rapid degradation of EV batteries due to increased charging and discharging cycles to send the surplus energy to the network. Both gaps are eliminated by developing a stand-alone and off-grid EV charging station as proposed in the current study.

Other studies have covered the utilization of Concentrated Photovoltaic-Thermal (CPV/T) and biomass energy in generating electricity but not for charging EVs. Since the literature review in solar PV and wind turbine hybridization in generating electricity for EV charging was already covered in the study (Al Wahedi and Bicer, 2019) by the author, this section adds on the previous studies conducted on utilizing CPV/T and biomass for generating electricity to identify the optimal renewable energy-based hybridization mix that can be used for the proposed case presented in this study.

CPV/T technology is a promising solution combining both CPV and thermal collectors where the undesirable thermal energy is harvested in a useful manner (Renno, 2014). It produces electricity and thermal energy, simultaneously reducing the costs of electricity production and increasing the overall use of solar energy (Alves et al., 2019). The generated heat is absorbed by circulating fluid embedded within PV panels, serving as a cooling mechanism to reduce panels' temperature which in turn enhances PV panels' electricity output efficiency, while the extracted heat by the fluid is used as useful input for subsequent subsystems. The cooling channels' shape and fluid flow rates must be selected carefully to ensure better heat transfer and uniform distribution of temperature on the receiver to avoid reaching maximum operating temperatures (85 °C) (Alves et al., 2019). The study of Salem et al. (2017) has compared a CPV/T system to uncooled PV cells where the electric and thermal efficiencies were found at 92% and 57.9% better, respectively. The experimental work by Yang et al. (2018) presents a CPV/T system in Nanjing, China, where the overall energy efficiency range was found from 55.6%–59%.

Interest in utilizing biomass as an alternative renewable resource for power generation has been increasing worldwide for the past several years. Biomass-based electricity production has many advantages, such as being a renewable source of energy, efficiently managing waste produced and not being subject to price fluctuations (Rodríguez-monroy et al., 2018). The global annual electricity production from biomass has risen from 227 TWh in 2004 to 646 TWh in 2016 (REN21 Secretariat, 2015, 2016). Biomass includes either waste streams, such as Municipal Solid Wastes (MSW), animal wastes and food processing wastes or aquatic plants including algae (Balat and Kirtay, 2010). Methods of biomass thermochemical and biological conversions into heat were developed for the past years as alternatives to fossil resources (Archer and Steinberger-wilckens, 2018). There are mainly four types of technologies through which electricity is generated from biomass: combustion, pyrolysis, gasification and anaerobic digestion as illustrated in Fig. 1. The first three technologies are thermo-chemical methods while the fourth one is a biological method (Suresh et al., 2019).

In combustion technology, biomass is burnt in the presence of air in a boiler and the generated heat is utilized by a power block to generate electricity (Suresh et al., 2019). Since the temperature and pressure of the steam generated by biomass boilers could reach up to 450 °C and 100 bar respectively (Modi and Haglind, 2014), steam Rankine cycle plants have been integrated in many studies with CPV/T subsystems to increase the efficiency

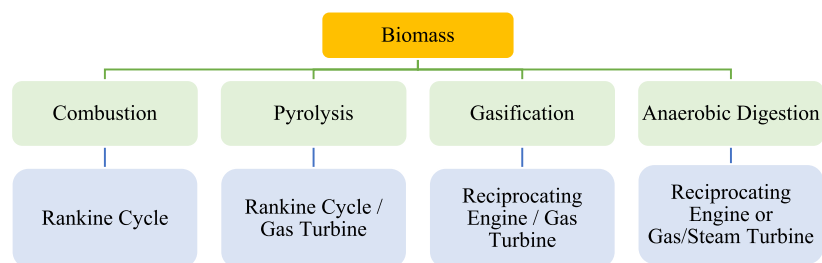


Fig. 1. Biomass power generation technologies.

of the overall system (Al-nimr et al., 2017). From the synergy point of view, CPV/T and biomass combustion technologies are a good combination for hybridization where many studies in the literature have assessed the integration of those technologies to generate electricity, especially for remote areas where stand-alone plants ranging from kW to GW scale can be implemented (Suresh et al., 2019). A parametric study for solar energy contribution for a 5 MW hybrid solar–biomass power plant was performed by Sahoo et al. (2016). The results showed an increase from 300 °C to 600 °C in steam temperature with 1.2 times increase in power output and increase in power block efficiency from 17.29% to 27%. Suresh et al. (2019) have modeled and analyzed a steam Rankine cycle based solar–biomass hybrid 20 MW power plant where results showed plant capacity utilization increased due to hybridization from 23% to 47%. The comparison made by Nixon et al. (2012) between hybrid solar–biomass power and biomass only plants has revealed that hybrid plants save up to 29% biomass and land with a cost range of 8.3–24.8 \$/GJ/a.

Since solar radiation availability is restricted during daytime and under favorable weather conditions, energy generation by PV panels is limited during those periods only. In addition, one of the main EV charging demand's characteristics is its stochastic nature resulting in underutilization of power generated by PV system during daytime due to a smaller number of EVs for charging compared to the generated power. To bridge the gap between the intermittent energy supply by PV panels and the stochastic EVs' energy demand, a need is triggered for integrating additional alternative RESs as well as suitable energy storage systems for continuous and reliable energy production (Khan et al., 2018).

Thermal energy is considered as one of the promising energy storage systems where thermal energy is stored in the form of sensible or latent heat. This is mainly in Phase Change Material (PCM) from which the energy can be retrieved when and as needed. The use of PCM, as per many studies, helps to improve the performance of PV systems (Renno, 2014). By introducing Thermal Energy Storage (TES) to a CPV/T plant, the unused thermal energy can be stored for later use, resulting in increasing the efficiency of the overall system. Moreover, adding PCM to CPV/T stabilizes temperature fluctuations caused by solar irradiance (Cui et al., 2016). In general, TES has higher efficiency and lower capital costs compared to other storage alternatives (Alves et al., 2019). Another means of storing energy is through chemical storage where electricity can be generated through fuel cells. H₂ and NH₃ are prominent examples of this type of storage system where the energy recovery efficiency reaches up to 70% (Bicer and Dincer, 2015; Larminie and Dicks, 2013). Electrochemical storage systems are other means of storing energy where the electricity can be generated directly once the storage is connected to the load. Batteries are considered the most famous type of electrochemical storage systems. In battery energy storage, energy recovery efficiency reaches up to 95% (Khan et al., 2019). However, one of the main drawbacks in using this technology is the batteries' performance and lifetime

dependency on operating temperature (Al-zareer et al., 2018). During charging and discharging processes, heat is generated due to electrochemical reactions and the battery's internal resistance to the flow of ions (Al-zareer et al., 2018). If the generated heat during those processes is not removed, the battery operating temperature will increase beyond the allowable operating temperature limits, which, in turn, will affect considerably the battery's performance (Al-zareer et al., 2019) and cause decreased battery lifetime (Al-zareer et al., 2018).

Due to longer life cycles and higher energy densities compared to other rechargeable battery types (Al-Zareer and Dincer, 2018), lithium-ion batteries are used in this study. As per the study by Pesaran (2002), temperatures between 25 °C and 40 °C are considered as acceptable operating temperatures for lithium-ion batteries. Higher or lower temperatures reduce the lifetime of the batteries due to film growth on the electrodes, which increases the internal resistance of lithium-ion batteries and reduces its lifetime (Qian et al., 2010). In high-temperature circumstances, there are mainly three types of cooling systems that can be used depending on the coolant type or phase, namely liquid cooling system, air cooling system and PCM cooling system (Al-zareer et al., 2018).

Although several studies have addressed the hybridization of RES and multiple energy storage facilities for supplying on-grid EV charging stations, only few have investigated similar hybridization for supplying off-grid EV charging stations. The design of a reliable stand-alone charging station comprises solar, wind and biomass RES along with electrochemical, chemical and thermal storage systems integrated with a cooling system has not been investigated before in literature. The scope of this study is to develop a hybridization system consisting of CPV/T, wind turbine, biomass combustion-based steam Rankine cycle integrated with battery, H₂, NH₃ and PCM storage units along with H₂ and NH₃ FCs and a cooling system for battery thermal management.

The rest of the paper is organized by presenting a case study and the specific objectives of this study followed by describing the developed design. Next, the criteria followed for selecting and sizing the main components of the design is explained, followed by design modeling and simulation to determine the optimal biomass plant size. Thermodynamic analysis of the developed design is performed next where the thermodynamic balance equations of the design's main subsystems and components are developed. The generated thermodynamic results are presented and discussed next, followed by the conclusion and future suggested works.

2. Scope and objectives

The State of Qatar has launched in May 2017 a sustainable initiative called "green car initiative" aiming to establish and expand the deployment of ecofriendly e-mobility across the country. A target was set to achieve 10% eco-friendly cars by 2030 which makes it a very challenging mission to realize considering the additional power demand required to supply the charging stations

and to avoid the associated consequences which were elaborated earlier in this paper.

The scope of this study is to develop an optimal renewable energy-based charging station design considering the site-specific conditions of Qatar in a sustainable manner. The study focuses on improving the overall system's efficiency and reliability of an earlier proposed design by the authors in study (Al Wahedi and Bicer, 2019) in which a hybrid PV and wind turbine subsystems, along with electrochemical and chemical storage facilities, were used in a grid-independent station to fast-charge a minimum of 50 EVs per day. This study aims to improve the previous design by:

- Replacing the PV system with CPV/T system to investigate the cooling effect in increasing PV panels' efficiency.
- Integrating thermal storage to utilize the generated thermal energy from CPV/T in a useful manner for feeding a cooling system.
- Incorporating a cooling system to maintain the electrochemical storage operating temperature within acceptable limits as well as liquefying and evaporating the produced ammonia in the design.
- Introducing a biomass-based steam Rankine cycle as an additional source of generating electricity to increase overall system's reliability and eliminate electricity shortage throughout the year.
- Increasing the charging capacity of a charging station by 60% to fast charge a minimum of 80 EVs per day instead of 50 EVs.

The specific objectives of this study can be summarized as follows:

- To design and develop a stand-alone renewable energy-based EV fast-charging station consisting of CPV/T, wind turbine and biomass combustion systems.
- Incorporating lithium-ion batteries, H_2 , NH_3 and PCM in the design as multiple sustainable energy storage alternatives along with H_2 and NH_3 Fuel Cells (FCs) to ensure uninterrupted charging operation during night times, cloudy days, and low wind speeds.
- Integrating a Li-Br absorption cooling system to cool down lithium-ion batteries for retaining their lifetime and at the same time for liquefying the produced gaseous NH_3 for safer storage purposes.
- To thermodynamically analyze the developed EV charging station design and assess the technical feasibility of the overall system.

The main novelty of this study is the optimal hybridization of three sources of renewable energy sources – namely CPV/T, wind and biomass technologies – complemented with three types of energy storage systems – namely electrochemical, chemical and thermal – to design a reliable and stand-alone fast-charging station supplying minimum 80 EVs per day in an eco-friendly manner with an internal cooling system for ammonia liquefaction and evaporation and battery cooling.

3. System description

The present study proposes a multigeneration stand-alone renewable energy-based fast-charging station where CPV/T, wind and biomass combustion technologies are integrated in a hybrid configuration for power generation along with multiple energy storage systems – namely battery, hydrogen, ammonia and PCM storage units as illustrated in Fig. 2. The plant has multiple modes of operation depending on solar, wind and biomass resources availability where the overall system can be divided into the following subsystems:

3.1. Concentrated Photovoltaic–Thermal (CPV/T)

CPV/T is one of the three main energy systems within the overall system, which produces both electricity and thermal energy. Energy is captured from the sun using concentrated PV panels and the produced electricity is used to fulfill the energy demand for hydrogen production process, EV charging, ammonia production and battery storage in a consecutive manner. If sufficient electricity is produced from CPV/T in a day, all the mentioned processes may be supplied with electricity from this subsystem. Otherwise, the first-in-order processes will be supplied until all the produced electricity from CPV/T is consumed and the other energy sources shall take over to supply the deficit. The produced thermal energy is used in the daytime for both charging PCM in the thermal storage unit and supplying the cooling system with the required heat energy.

3.2. Wind turbine

Wind turbine is the second main energy system within the overall system, where the produced electricity is used for EV charging and battery charging subsequently. Energy is captured from the wind by means of horizontal axis wind turbine. The advantage of this subsystem over the CPV/T is its ability to produce electricity even during night times, as long the available wind speed is within the desired limits.

3.3. Biomass-based steam Rankine Cycle

This subsystem is used to complement the other sources during night times and unfavorable weather conditions where the generated heat by biomass combustion is used for heat addition process in steam Rankine cycle for electrical power generation. Steam Rankine cycle is coupled with a biomass combustion subsystem to generate the required electricity for meeting the shortfall demand during unfavorable periods. The size of this system is kept minimal to use solar and wind energy as much as possible. This subsystem can also be replaced with a biodiesel generator as back-up power source.

3.4. Hydrogen production and hydrogen fuel cell

This subsystem consists of an electrolyzer, H_2 FC, H_2 , O_2 and H_2O storage tanks. H_2 FC is given priority among other storage systems to produce electricity in case solar and wind electricity production is not sufficient to meet the required demand.

3.5. Ammonia production and ammonia fuel cell

This subsystem consists of an air separation unit, Haber–Bosch NH_3 production, NH_3 FC, NH_3 , and O_2 storage tanks. NH_3 FC is given second priority among other storage systems to produce electricity in case solar and wind electricity production is not sufficient to meet demand shortage.

3.6. Battery storage system

This energy storage subsystem is given third priority after the above two energy storage subsystems in terms of supplying energy shortage not fulfilled by all other main sources and storage systems.

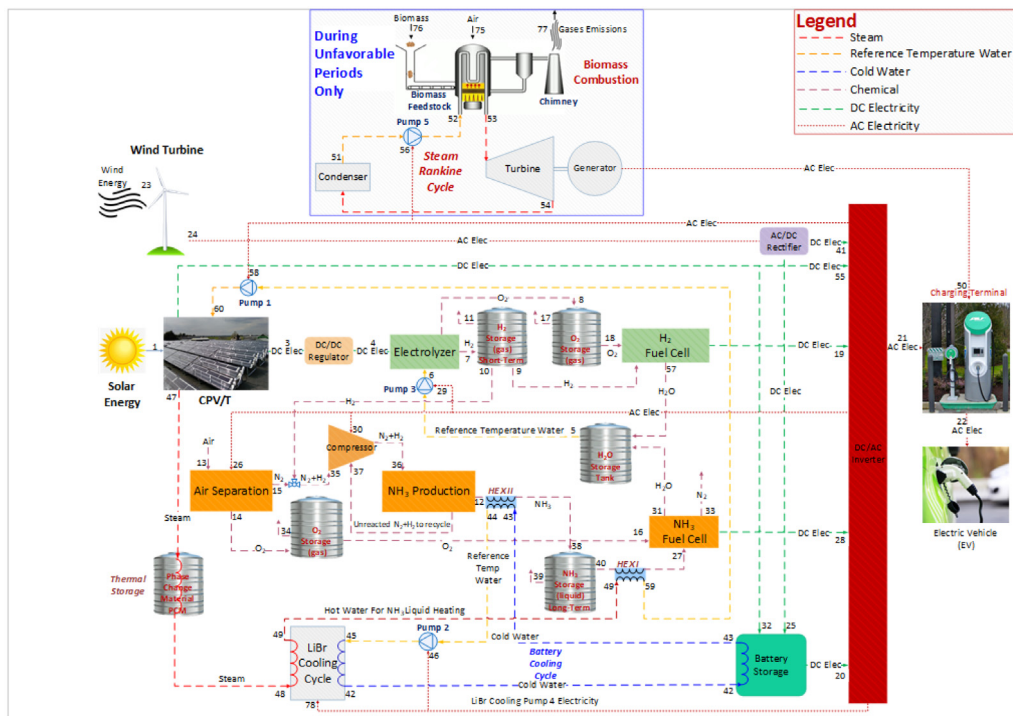


Fig. 2. Schematic diagram of the proposed stand-alone renewable energy-based EV charging station.

3.7. Thermal Energy Storage (TES)

A latent heat based TES unit is incorporated within the system where Hydrated Salt S89 is used as suitable PCM, based on the required temperatures in the system (Phase Change Material Products Limited, 2013). TES is continuously charged during the daytime and discharged during night times. The main purpose of this thermal energy storage subsystem is to secure the thermal energy required during the night and unfavorable periods to ensure an uninterrupted supply of hot stream to the LiBr cooling system.

3.8. Li-Br Absorption Cooling System (ACS)

To retain the lifetime of the battery storage as well as providing the necessary cooling process to store the produced NH_3 in liquid form, a Li-Br absorption cooling subsystem is incorporated in the design.

3.9. Circulating pumps

Pumps 1, 2, 3, 4 and 5 are used to circulate hot water in CPV/T cycle, cold water in the battery and NH_3 cooling cycle, water in electrolysis process, Heat Transfer Fluid (HTF) in Li-Br ACS cycle and water in steam Rankine cycle respectively.

4. Selection and sizing

Assuming the land space dedicated for the charging station should not exceed $1,500 \text{ m}^2$ and the average power required to charge an EV is 35 kWh (Al Wahedi and Bicer, 2019), PVSyst software (PVsyst 6.7.8 software, 2018) is used for selecting the optimum CPV/T plant for the system inclusive of battery storage and inverter. Technical specification data of the selected components extracted from PVSyst are reflected in Table 1. The data of the initial design parameters are listed in Table 2.

Next, considering the meteorological conditions of the State of Qatar and space limitations, the optimal size of the wind turbine

Table 1

Technical specifications of CPV/T, inverter and battery storage system.

PV module	
Cell type	GalnP2/GaAs/Ge
Model	CX-M500 1.00.086
Manufacturer	Soitec
Operating temperature	50°C
Number of PV modules	1 in series and 191 in parallel
Rating	468 kWp
Average daily profile	1728 kWh
Total area	1497 m^2
Inverter	
Model	AGILO 75.0-3 Outdoor
Manufacturer	Fronius International
Number of inverters	5 units
Battery	
Model	Powerwall
Manufacturer	Tesla
Operating temperature	20°C
Number of units	6 in series x 20 in parallel
Stored energy	654.0 kWh

is selected from the market (EWT DW, 2020). About 40% of the total produced electricity from CPV/T unit is used for H_2 production; about 40% is used for EV charging and about 20% is used for battery charging. Installed capacity of about 200 kW is selected as the optimal capacity to be generated by both hydrogen and ammonia FCs. The associated power and storage requirements are calculated using Engineering Equation Solver (EES) software.

5. Design, modeling and simulation

As the incorporated CPV/T and wind turbine ratings, along with energy storage capacities, are determined by earlier steps, the next step is to develop an interactive simulation model to assess the optimal steam turbine capacity to cover the demand shortage not fulfilled during unfavorable weather conditions. The model is designed such that the steam turbine capacity can be

Table 2
Main design parameters used in the analysis.

Parameter	Description/Value	Reference
CPV/T		
Average energy production	1728 kWh/day	PVsyst 6.7.8 software (2018)
Installed area	1497 m ²	PVsyst 6.7.8 software (2018)
Li-ion Batteries		
Storage capacity	654 kWh	PVsyst 6.7.8 software (2018)
Total battery storage weight	11640 kg	PVsyst 6.7.8 software (2018)
PCM		
PCM type	Hydrated Salt S89	Phase Change Material Products Limited (2013)
Phase change temperature	89 °C	Phase Change Material Products Limited (2013)
Latent heat capacity	151 kJ/kg	Phase Change Material Products Limited (2013)
Wind turbine		
Installed capacity	250 kW	Wind-turbine models.com (2020)
Model	EWT DW 54–250	Wind-turbine models.com (2020)
Axis type	Horizontal	Wind-turbine models.com (2020)
Cut-in wind speed	2.5 m/s	Wind-turbine models.com (2020)
Rated wind speed	7.5 m/s	Wind-turbine models.com (2020)
Cut-out wind speed	25 m/s	Wind-turbine models.com (2020)
Wind turbine rotor diameter	54 m	Wind-turbine models.com (2020)
Wind turbine lambda (λ)	0.65	–

altered for the purposes of simulating and evaluating different capacities based on how the optimal steam turbine sizing can be determined.

Based on the data extracted from PVsyst for the selected CPV/T, the daily power curves are modeled using the developed model. Similarly, wind data obtained from HOMER are used as input for equations to calculate the hourly power generated by the selected wind turbine and the daily power curves are modeled as well. The daily profile modeling generated from PVsyst for the CPV/T system for randomly selected days are compared with the ones generated from the developed model for the same respective days and they are both found identical. Similarly, the daily profile modeling generated from HOMER for the wind turbine for randomly selected days are compared with the ones generated by the developed Excel model for the same corresponding days and both are found identical as well. Fig. 3 depicts both CPV/T and wind daily profiles generated from the developed Excel program for a randomly selected day in April.

The daily load demand for charging 80 EVs with a total load of 2,800 kWh is represented by a stochastic modeling curve extrapolated from the study (Bayram et al., 2016) where a realistic daily demand profile of EVs arriving at the charging station was considered. Fig. 4 illustrates the stochastic profile used in this study to represent the daily EV demand.

In order to determine the hourly energy produced and consumed in a day, algorithms are developed based on the main constraints indicated in Table 3. For the optimum control mechanism of the complete system, the priority hierarchy levels indicated in Fig. 5 are utilized.

Next, Visual Basic programming code in Excel software is used to calculate the daily produced and consumed energy for a complete year. Based on the developed optimization program, about 33 kW biomass-driven steam turbine is the optimal size to be incorporated in the stand-alone design to eliminate supply shortage and fulfill the daily EV demand in a reliable manner

Table 3
Main constraints in the optimization process.

Constraints	Value
Solar intermittency	Hourly irradiation from PVsyst
Wind intermittency	Hourly wind speed from HOMER
Space limitation	1,500 m ²
Minimum charging points	4
Energy per single EV charging	35 kWh

throughout the year. Fig. 6 illustrates simulation results of a typical day in April where RES and load profiles along with the associated results are presented.

The daily solar profile is extracted from the PVsyst program (PVsyst 6.7.8 software, 2018) while the daily wind turbine profile is extracted from HOMER Pro program (The HOMER, 2018). The daily load demand for charging 80 EVs is represented by a stochastic modeling curve extrapolated from a realistic daily demand profile for EVs arriving at the charging stations, which is taken from a literature study (Bayram et al., 2016).

6. Thermodynamic analysis

The thermodynamic analysis approach followed in this study is based on conducting a detailed thermodynamic assessment of the whole system proposed in Fig. 2. The first step is to formulate the balance equations for each component individually based on thermodynamic laws related to mass, energy, entropy, and exergy. Next, all the equations are developed and interlinked in EES software (EES, 2018) using appropriate codes based on the assigned state points for each component in the overall system. Finally, the derived results from EES are assessed and discussed.

The thermodynamic analysis of the proposed system is based on the following assumptions:

- Steady-state steady flow operations exist for all components.
- Reference pressure and temperature are 101.3 kPa and 25 °C, respectively.
- Kinetic and potential terms are neglected for all components except the wind turbine (Rabbani et al., 2012).
- The average sun irradiance intensity is 700 W/m².
- Sun temperature is assumed to be 6000 °C.
- The average wind speed is 5.6 m/s as calculated from the data obtained from (Méndez and Bicer, 2019) where only wind speeds between the cut-in speed and cut-out speed of the selected wind turbine are considered.
- The average wind blowing hours per day is assumed to be 12 h.
- Wind turbine transmission and generator efficiencies are 95% (Cadu et al., 2012).
- AC–DC and DC–AC inverter's efficiencies are taken as 95% (Notton, 2010).
- Battery charging and discharging efficiencies are taken as 95%.
- Thermal storage charging and discharging efficiencies are taken as 95%.
- The average sun hours and thermal storage charging period during the daytime are 8 h.
- The thermal storage discharging period during nighttime is 16 h.
- The water pump and ammonia production unit operate on average for 8 h per day.
- Hydrogen and oxygen gases have about 10% leakage and boil-off gas losses from the storage tanks.
- Pumps and steam turbine isentropic efficiencies are 85%.

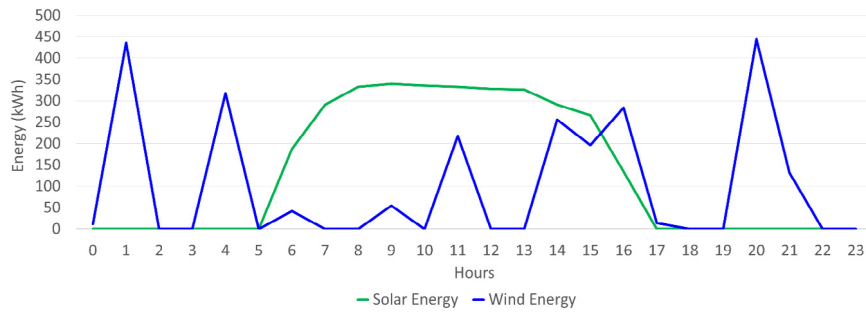


Fig. 3. CPV/T and wind daily energy generation profiles in Qatar based on the considered capacities for a randomly selected day in April.

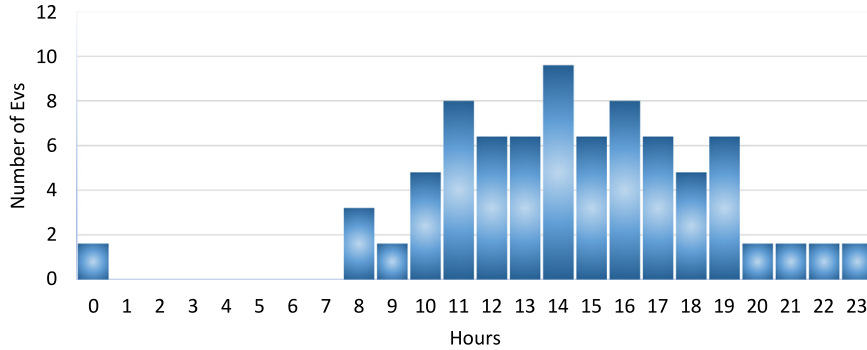


Fig. 4. Extrapolated stochastic daily EV demand profile.

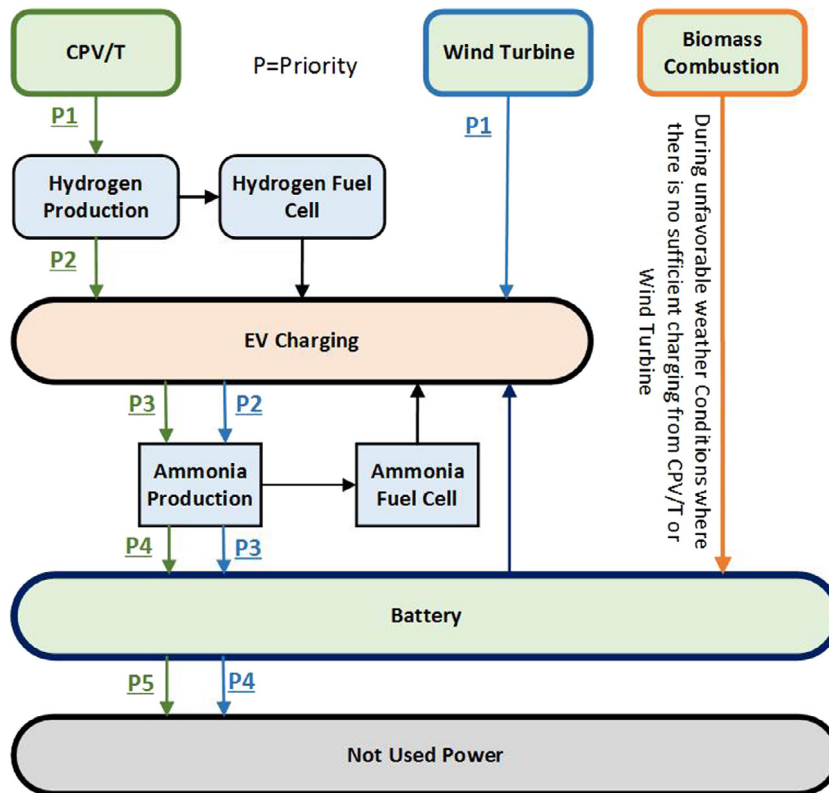


Fig. 5. Priority hierarchy level considered in the control strategy of the proposed charging station.

- CPV/T electrical efficiency is 35% (Daneshzarian et al., 2018).
- Li-ion battery specific heat capacity at 50 °C and 35 °C is 0.84 kJ/kgK and 0.82 kJ/kgK, respectively (Inforlab Chemie, 2010).

Table S1 in the supplementary file contains all the thermodynamic balance equations along with energy and exergy efficiency equations of the main subsystems and components incorporated in the design. Eq. (1) sums up the total electricity consumption by

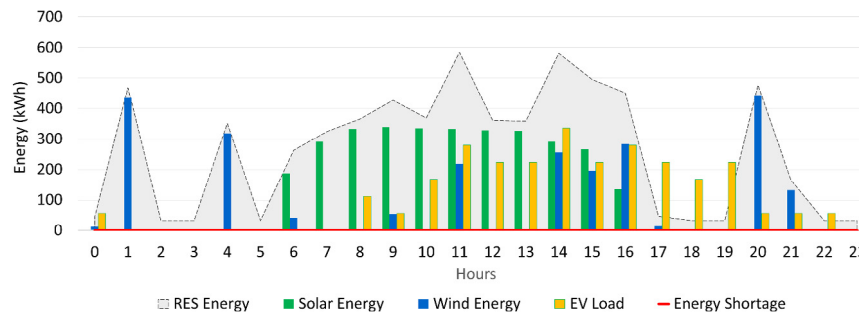


Fig. 6. Modeling and simulation results for a typical day in April in Qatar.

the incorporated components to operate the overall station while the total charging power inclusive of electricity generated by the steam turbine is computed by Eq. (2).

$$\dot{W}_{\text{Total Electrical Consumption}} = \dot{W}_{\text{Pump1}} + \dot{W}_{\text{Pump2}} + \dot{W}_{\text{Pump3}} + \dot{W}_{\text{Pump4}} + \dot{W}_{\text{Pump5}} + \dot{W}_{\text{AirSeparator}} + \dot{W}_{\text{NH}_3\text{Compressor}} \quad (1)$$

$$\dot{W}_{\text{Charging TOTAL}} = (\dot{W}_{\text{Wind}} + \dot{W}_{\text{BatteryWithCooling}} + \dot{W}_{\text{out,CPVT}} + \dot{W}_{\text{el,NH}_3\text{FCout}} + \dot{W}_{\text{el,H}_2\text{FCout}} + \dot{W}_{\text{Biomass}} - \dot{W}_{\text{Total Electrical Consumption}}) \times \eta_{\text{DCACInverter}} \times \eta_{\text{Charging Terminal}} \quad (2)$$

Eqs. (3) and (4) given in Box I define the energy and exergy efficiencies of the overall system, respectively.

To analyze the complete system in EES software, the equations given here and in Table S1 are encoded in EES by assigning proper state points as indicated in Fig. 2 for each component. The derived results and generated plots by EES are discussed in the following section.

7. Results and discussion

To assess the performance of the proposed system, comprehensive energy and exergy investigations are performed. Based on the analysis performed using EES software of the proposed system, the thermodynamic properties, such as mass flow rates, temperatures, pressures, specific enthalpies, specific entropies and specific exergies of the subsystems at each state point, are determined.

The energy efficiencies of the subsystems and main components are calculated to assess the overall system performance. The energy efficiencies of each sub-system and the overall system under normal operating conditions are computed and depicted in Fig. 7.

The energy efficiencies of H_2 and NH_3 fuel cells are found to be 77% and 72%, respectively, which are relatively at a higher end compared to literature review (Bicer and Dincer, 2015; Larminie and Dicks, 2013). The energetic COP of ACS is found to be 0.72, which is within a good range compared to results achieved by similar studies (Usman Sajid and Bicer, 2020). The CVP/T thermal efficiency is found to be 45%, which is within good range compared to literature review (Gholami et al., 2015). The overall energy efficiency of the integrated system is found to be 45%, which is relatively in the higher range compared with achieved results by other RES based multi-generation systems in the literature (Ghasemi et al., 2018).

Similarly, the exergy efficiencies are calculated for the subsystems and components as shown in Fig. 8. The exergy efficiencies of the subsystems and components are different than energy efficiencies, implying that, through exergy analysis, a deeper analysis is possible where non-recovered part of exergy is denoted as exergy destruction. The exergy efficiency of the CPV/T plant is found to be 37% whereas wind turbine exergy efficiency is found

Table 4

The exergy destruction rates of the components and sub-systems.

Component/Subsystem	Exergy destruction rate (kW)
Air separation	0.581
NH_3 production	2.690
NH_3 storage	0.013
NH_3 fuel cell	7.052
Electrolyzer	46.610
H_2 storage	0.167
H_2 fuel cell	11.420
Biomass combustion	50.990
CPV/T	539.800
Turbine	5.313
PCM storage	2.140

to be 43%. The exergetic COP of ACS is found to be 0.19, which is within a good range compared to results achieved by similar studies (Khan et al., 2018) while the exergy efficiency of the battery cooling cycle is found to be 57%. The overall exergy efficiency of the integrated system is found to be 19%, which is relatively in the higher range compared to achieved results by other RES based multi-generation systems in the literature (Ghasemi et al., 2018). Further analysis is performed through evaluating the values of exergy destruction, heat rates, work rates, and energy production quantities of each subsystem.

In Table 4, the exergy destruction rates of the main components and subsystems are listed, where the highest exergy destruction occurs in the CPV/T plant due to huge heat losses and relatively lower energy conversion efficiency. The biomass combustion and electrolyzer for hydrogen production have the second and third highest exergy destruction rates among other subsystems. The exergy destruction rates of H_2 and NH_3 fuel cells are found to be 11.42 kW and 7.052 kW, respectively.

Table 5 reflects the heat rate (heat inputs or outputs) values of selected subsystems. Due to the large size of CPV/T, the total heat input was relatively high, reaching 1047 kW, and the respective losses were large as well, reaching 202.1 kW. The fuel cells' heat generation values were 19.57 kW and 1.5 kW for H_2 and NH_3 fuel cells, respectively.

The work rates generated by the multiple energy sources incorporated in the system are shown in Table 6. Solar energy has the dominant share with 366.5 kW total work rate, however, due to its intermittent nature and stochastic EV demand, only 146.6 kW is used for EV charging directly while the rest is stored in electrochemical and chemical form for nighttime and unfavorable time consumption. Battery system and wind turbine had the second and third highest share with 118.3 kW and 97.47 work rate, respectively, followed by H_2 FC with a 52.74 kW work rate. Similar to CPV/T, wind work rate contribution for direct EV charging, due to its intermittent nature and stochastic EV demand, is 46.3 kW, which is 50% of its total production capacity, while the rest is used for charging the battery storage. The steam turbine work rate comes next with 46.23 kW since it used during unfavorable

$$\eta_{en} = \frac{(\dot{W}_{Total \text{ Charging}} - \dot{W}_{Total \text{ Electrical Consumption}} + \dot{m}_{H_2O,in} \cdot h_{H_2O,in} - \dot{m}_{H_2O,out} \cdot h_{H_2O,out})}{\dot{Q}_{in,CPVT} + \dot{W}_{in,Wind} + \dot{m}_{biomass} HV_{biomass}} \quad (3)$$

$$\eta_{ex} = \frac{(\dot{W}_{Total \text{ Charging}} - \dot{W}_{Total \text{ Electrical Consumption}} + \dot{m}_{H_2O,in} \cdot ex_{H_2O,in} - \dot{m}_{H_2O,out} \cdot ex_{H_2O,out})}{\dot{Q}_{in,CPVT} \left(1 - \frac{T_0}{T_{sun}}\right) + \dot{W}_{in,Wind} + \dot{m}_{bio} \cdot ex_{bio}} \quad (4)$$

Box 1.

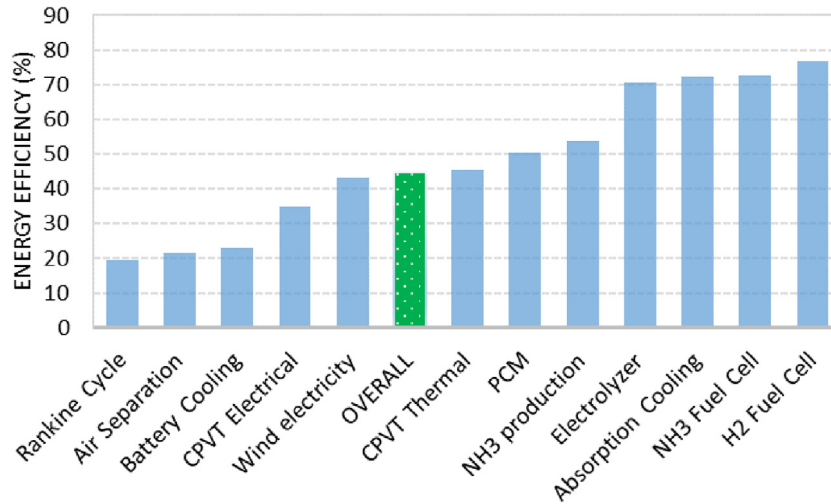


Fig. 7. The energy efficiencies of the sub-systems and the overall system.

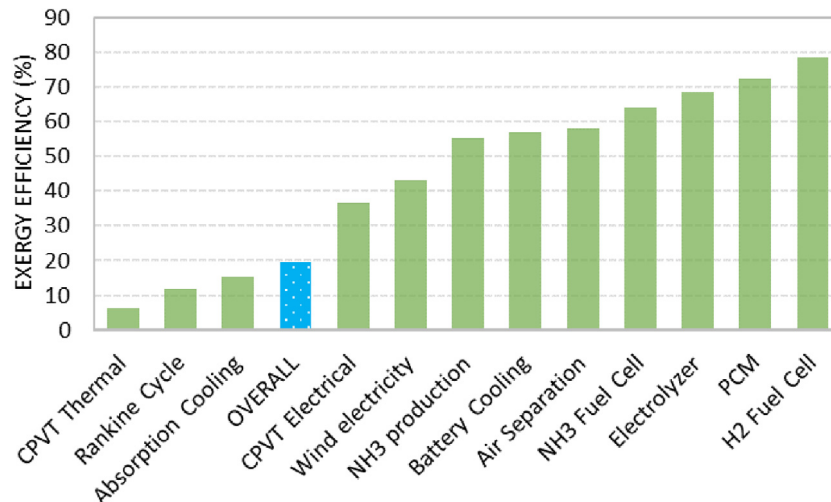


Fig. 8. The exergy efficiencies of the sub-systems and the overall system.

weather conditions only. Although the project is mainly designed for electricity production for EV charging, incorporated sub-systems' components, such as pumps, electrolyzer, compressor and air separation, also require electricity, which is secured by the system. Even though 628.5 kW work rate is generated, 381.6 kW is the net work rate utilized for EV charging.

Based on the designed operating hours for the different sub-systems and components, Table 7 represents the daily energy produced by each subsystem for EV charging. To observe the performance of the overall system and subsystems, due to changes of some crucial parameters such as solar irradiance, wind speed and ambient temperature, various parametric studies are performed

by changing the values of selected variables and observing the behavior of the associated parameters. Similarly, to understand the effects of varying the certain parameters such as water flow rate, biomass rate, N₂ flow rate and battery weight, parametric studies are performed and the results are evaluated.

Fig. 9 depicts the changes in CPV/T generated useful heat and heat loss based on water flow change from 0.8 to 1.7 kg/s. The result showed the increase of flow rate increases the amount of generated useful heat while the heat loss decreases as heat absorbed by the HTF. Accordingly, increasing the CPV/T pump

Table 5

The heat rates of the sub-systems.

Description	Heat rate (kW)
CPV/T input	1047
CPVT loss	202.1
CPV/T useful heat output	478.5
Cooling capacity	69.55
Electrolyzer	45.19
H ₂ fuel cell	19.57
HEXI	175.6
HEXII	0.775
NH ₃ fuel cell	1.529
PCM storage	101.5
Battery cooling	16.13

Table 6

The work rates of the sub-systems.

Description	Work rate (kW)
Battery with cooling	118.3
Wind turbine (for battery storage)	46.3
Wind turbine (for EV charging)	46.3
H ₂ fuel cell	52.74
NH ₃ fuel cell	15.29
Steam turbine	46.23
CPV/T (for battery storage)	73.3
CPV/T (for H ₂ FC)	146.6
CPV/T (for EV charging)	146.6

Table 7

Daily produced and consumed energy by the sub-systems and the overall system.

Description	Energy (kWh)
Produced Energy	
Battery system	648
Wind turbine (for EV charging)	556
H ₂ fuel cell	422
NH ₃ fuel cell	122
CPVT (for EV charging)	1,172.80
Total produced energy	2,920.64
Consumed Energy	
CPV/T HTF pump	3.36
Battery cooling pump	0.94
Electrolyzer pump	0.03
LiBr cooling pump	0.01
Air separation	11.00
NH ₃ production compressor	152.88
Total consumed energy	168.21
Net energy	2,752.43

flow rate increases both CPV/T's energetic and exergetic efficiencies but the generated heat shall be used in a useful manner to increase the overall system energetic and exergetic efficiencies.

Since solar irradiation is a varying parameter throughout the year, hence, another parametric study is conducted to investigate the effects of solar irradiation change from 300 to 1200 W/m² on the CPV/T output as shown in Fig. 10. Solar irradiance has a dominant effect on increasing the electricity output of the PV panels thus increasing the generated electricity by the CPV/T. With the increase in the irradiance, the total power output from CPV/T increases gradually, but the exergy destruction increases dramatically. Comparing with 366.5 kW generated power from the CPV/T plant at 700 W/m² solar irradiance, 500 kW is generated at 1,000 W/m² solar irradiance, as illustrated in Fig. 10. This allowed more hydrogen and ammonia generation, storage battery charging and EV charging capabilities.

The effects of wind speed changes from 1 to 11 m/s are studied as shown in Fig. 11. The wind velocity has a dominant effect on increasing the electricity output of the wind turbine thus increasing the generated electricity by the wind turbine. Although the overall energy efficiency of the system decreases from 48%

to 43% when wind speed raises from 3 m/s to 9 m/s, the overall exergy efficiency increases from 22% to 28% as shown in Fig. 11.

Another parametric study is conducted on the mass rate of the biomass feed rate supplied to combustion process, where the generated heat is used for the constant pressure heat addition process in the steam Rankine cycle. The heat generated and the overall system efficiency are investigated under various biomass feed rates as shown in Fig. 12.

As biomass feedstock rate increases, the heat generated by the combustion process increases as well as the exergy destruction. Both the overall system energy and exergy efficiencies decrease as biomass feedstock rate increases.

The impact of reference temperature change on FCs is examined to observe its impact on the selected parameters. The increase of reference temperature decreases H₂ FC exergy efficiency while both overall energy and exergy efficiencies decrease as illustrated in Fig. 13. The increase of reference temperature increases NH₃ FC exergy destruction while both NH₃ FC and overall exergy efficiencies decrease as illustrated in Fig. 14. These two parametric studies prove that the exergy efficiency is considerably dependent on the reference temperature.

The effects of operating temperature change on FCs are investigated to observe its impact on useful work produced, exergy destruction and exergy efficiency. For H₂ FC, operating temperature rise increases the work produced slightly and decreases the exergy destruction while the exergy efficiency increases considerably as shown in Fig. 15.

For NH₃ FC, operating temperature rise increases the work produced and decreases the exergy destruction while the exergy efficiency increases as shown in Fig. 16. These two parametric studies conclude that the operating temperature rise has a positive effect by increasing the work production and exergy efficiency of FCs while decreasing the exergy destruction.

Water flow rate change in the steam Rankine cycle is examined against useful work and exergy destruction generated by the steam turbine as well as the overall system energy and exergy efficiencies. As per Fig. 17, the results show that increasing the flow rate increases the generated work considerably that is accompanied by a sizable increase in the exergy destruction rate and the overall energy and exergy efficiencies.

Although the available cooling capacity generated from the Li–Br water absorption cooling system is 69.55 kW, the utilized cooling capacity for the battery cooling (11,640 kg Li-ion battery system) is only 16.14 kW. The rest is used for liquefaction purposes. A parametric study is conducted to evaluate the impact of selected battery system weight on increasing the utilization of available cooling capacity in battery cooling process and the associated battery cooling energy and exergy efficiencies. As per Fig. 18, battery systems with higher weights can benefit more from the available cooling capacity, increasing the energy and exergy of the battery cooling system. This is due to the fact that increasing the mass of the battery is directly proportional to the amount of heat generated by the battery during the charging and discharging process, which in turn increases the amount of heat absorbed by the cooling system. This leads to an increase in the energy and exergy of the battery cooling system.

The impacts of changing the water flow rate to electrolyzer are examined to observe its effects on various selected parameters. Fig. 19 shows the results of this investigation on generated useful work, the exergy efficiencies of H₂ FC and the overall system. Increasing the mass flow rate considerably rises the generated work. Both H₂ and overall system's efficiencies increase as well.

Finally, the effects of changing the N₂ mass flow rate change in the NH₃ production process are investigated on the generated power by NH₃ FC, exergy destructions of NH₃ compressor, NH₃ production, and exergy efficiency of the overall system. As shown

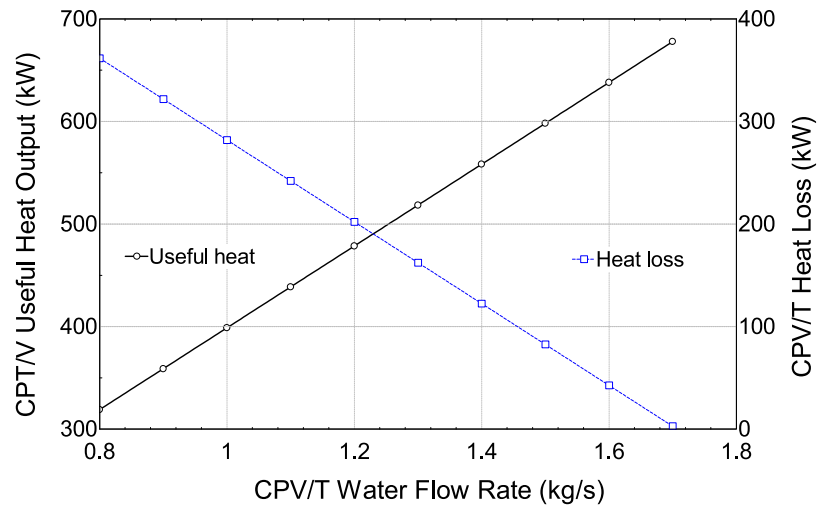


Fig. 9. The effects of CPV/T water flow rate on the produced useful thermal energy and heat loss.

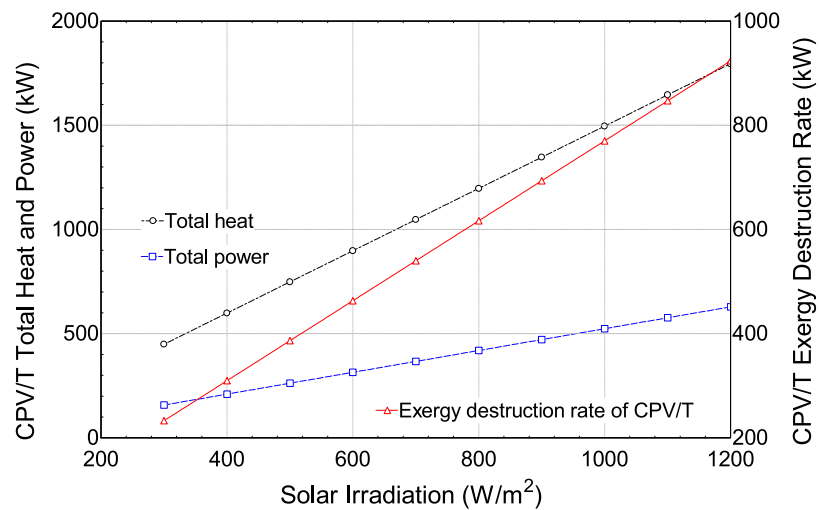


Fig. 10. The effects of the solar irradiance on the electrical output and exergy destruction rates of CPV/T.

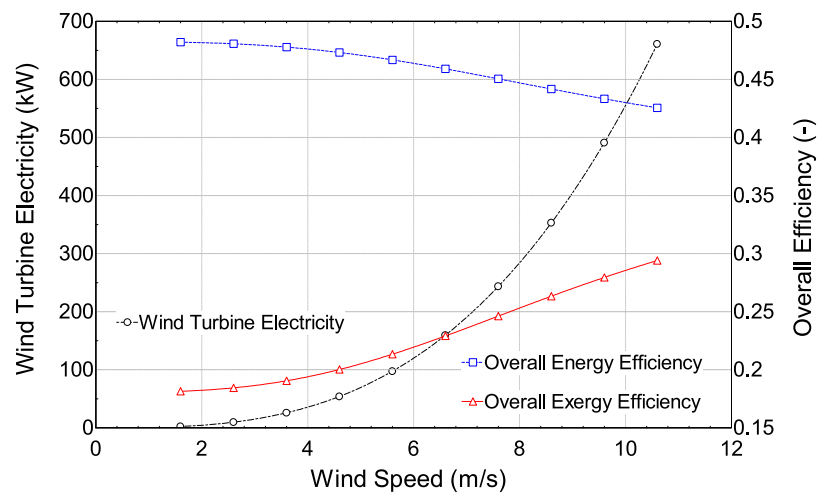


Fig. 11. The effects of the wind speed on the electrical output of wind turbine and overall efficiencies.

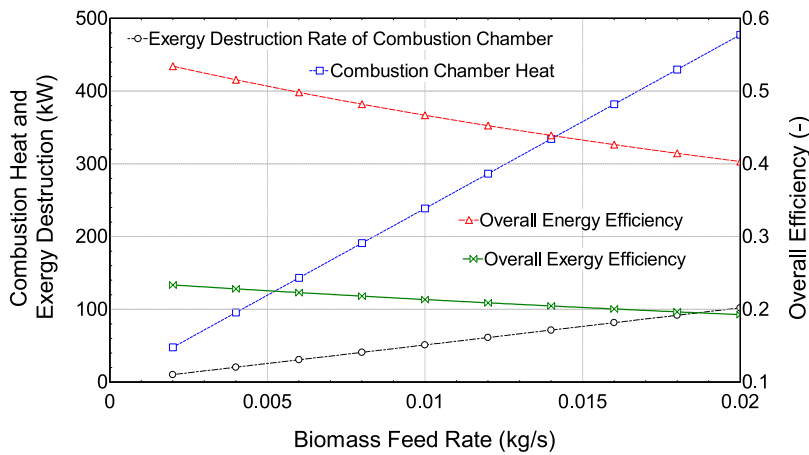


Fig. 12. The effects of biomass feed rate on the heat generation and the overall efficiency.

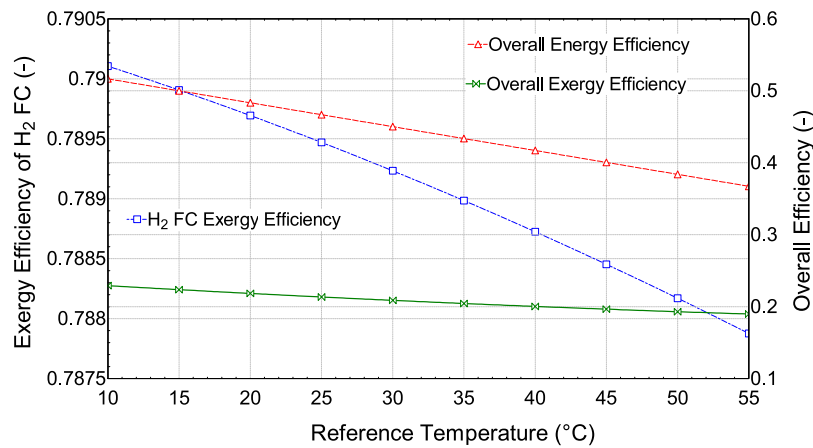


Fig. 13. The effects of the reference temperature on the H₂ FC and the overall system performance.

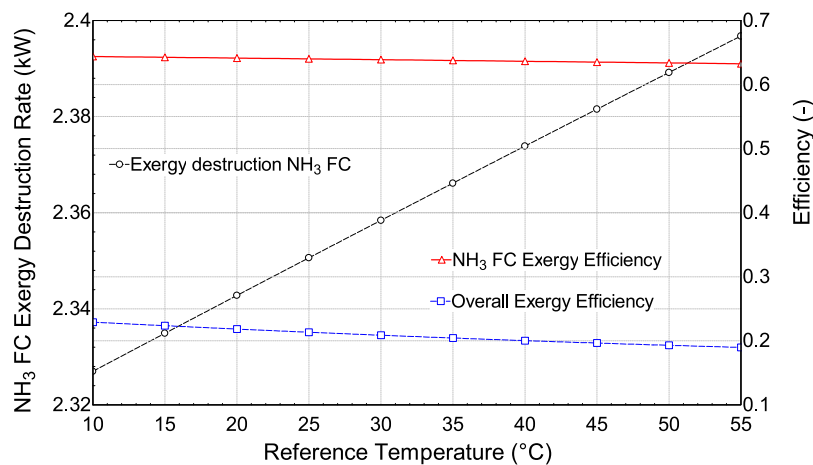


Fig. 14. The effects of the reference temperature on the NH₃ FC and the overall system performance.

in Fig. 20, increasing the N₂ mass flow rate increases considerably the generated work by NH₃ FC and the exergy destruction for both NH₃ compressor and NH₃ production increase as well, while the overall system exergy efficiency decreases slightly.

8. Conclusions and future work

The main objective of this study is to propose an eco-friendly stand-alone fast EV charging station running on purely hybrid

RES. The contribution of this study is to propose a reliable and grid-independent combined solar, wind and steam Rankine cycle plant heated by biomass combustion chamber along with battery, hydrogen, ammonia and thermal storage systems to fast-charge 80 PEVs per day. The detailed thermodynamic assessment is performed using parametric studies in EES for the proposed design, considering the site specific conditions and intermittency nature of RES, and it has proven the reliability of the proposed system to fulfill the targeted objectives in the State of Qatar which is

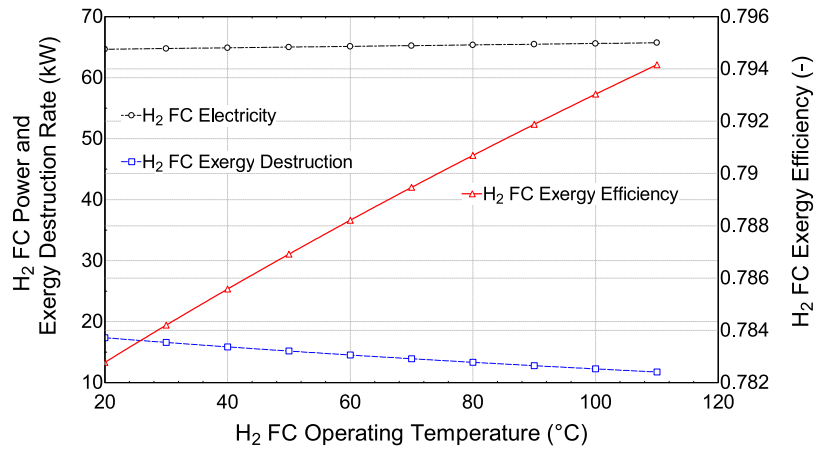


Fig. 15. The effects of H_2 FC operating temperature on the power production, exergy destruction and exergy efficiency of H_2 FC.

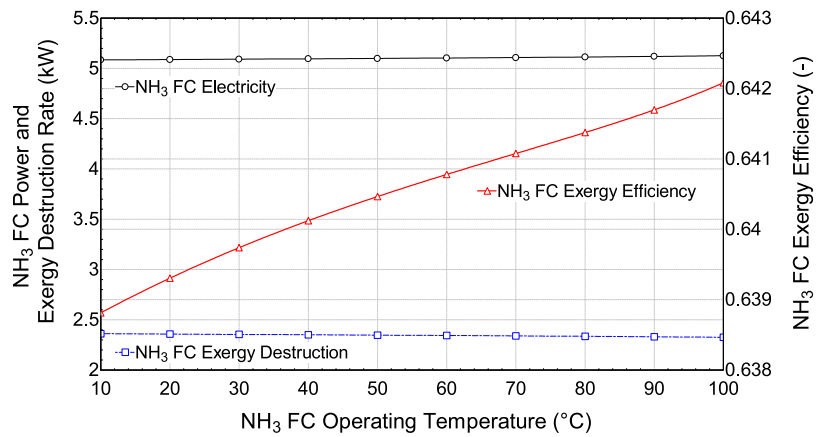


Fig. 16. The effects of NH_3 FC temperature on the power production, exergy destruction and exergy efficiency of NH_3 FC.

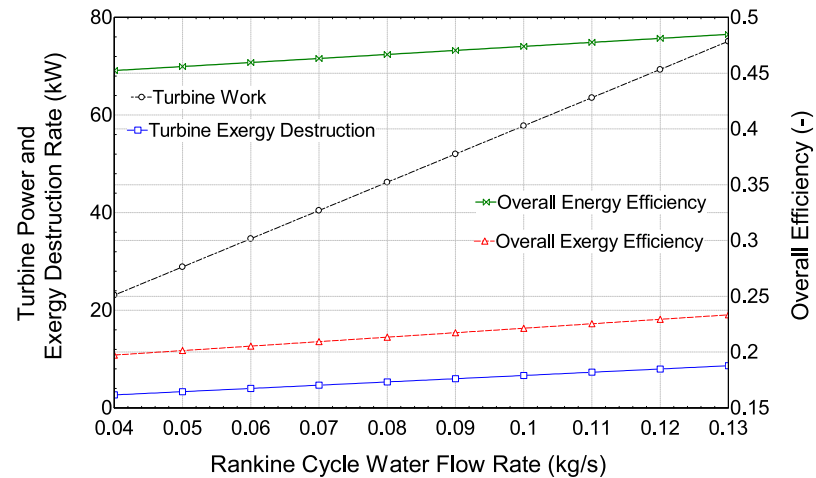


Fig. 17. The effects of steam Rankine cycle water flow rate on turbine's work, exergy destruction rate and overall system efficiencies.

located in a hot and arid region. The impacts of several significant operating parameters, such as battery capacity, solar irradiation, wind speed, and ambient temperature, are investigated to find out the optimal configuration and operational mode. The main results of the study are summarized as follows:

- The overall system energy and exergy efficiencies are found to be 45% and 19%, respectively.
- The energy efficiencies of H_2 and NH_3 fuel cells are found to be 77% and 72%, respectively.
- The energetic and exergetic COP of ACS is found to be 0.72 and 0.19, respectively.
- The CVP/T thermal efficiency and electrical exergy efficiency are found to be 45% and 37%, respectively.
- The heat generated by CPV/T is utilized by integration with an Li-Br absorption cooling system which is utilized for liquefying the produced NH_3 gas prior to storage and for

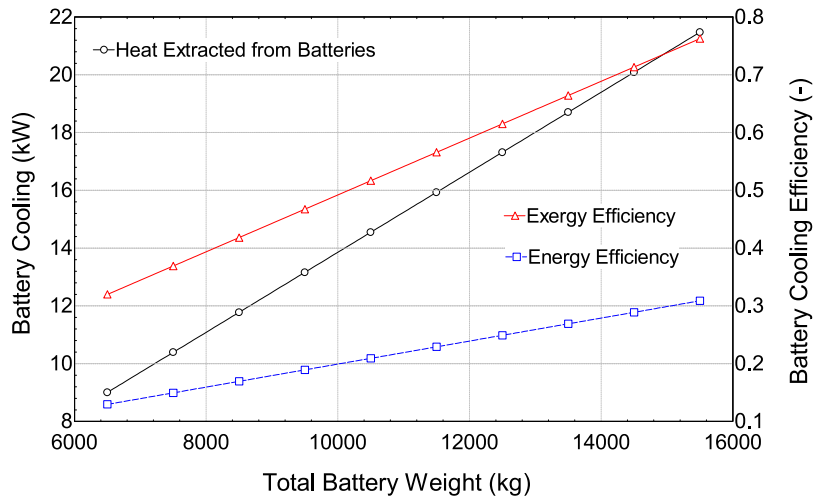


Fig. 18. The effects of battery system weight on the cooling capacity and the efficiencies of battery cooling.

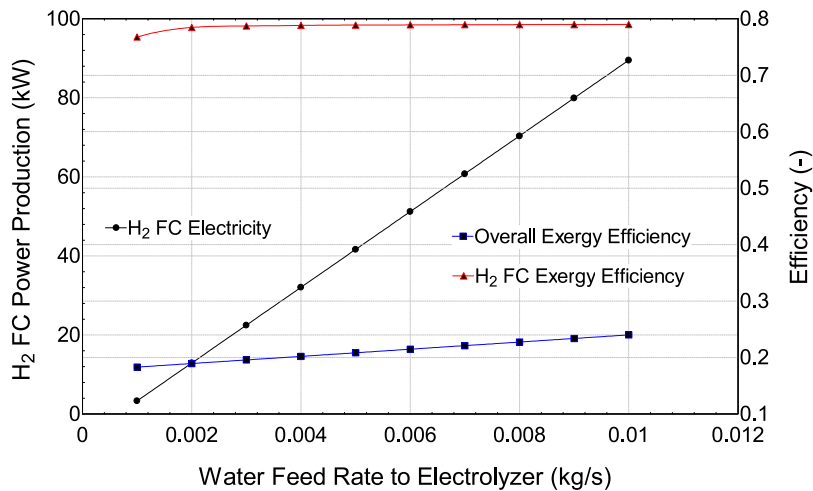


Fig. 19. The effects of electrolyzer water flow rate on H₂ FC power and the efficiencies of H₂ FC, and the overall system.

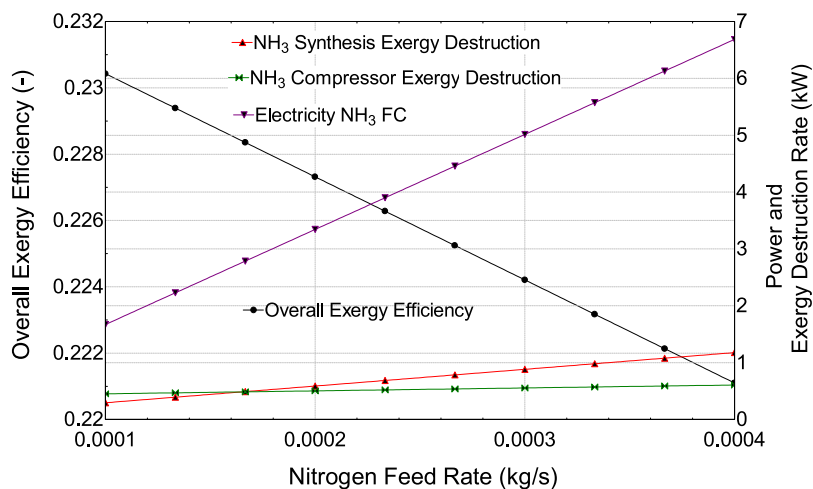


Fig. 20. The effects of N₂ flow rate on NH₃ FC power, NH₃ compressor exergy destruction, NH₃ production process exergy destruction and overall system exergy efficiency.

cooling the battery storage system to maintain the operating temperatures below 50 °C to retain its lifetime.

- A PCM thermal storage system is incorporated as well to maintain hot water flow to the absorption cooling system during night times and unfavorable weather conditions.

To further improve the overall efficiency of the system, the heat loss generated from CPV/T can be utilized for several applications such as hot water, space heating and cooling in future projects. Moreover, increasing the CPV/T water flow rate increases the generated heat energy which can be used for the suggested purposes as well. Detailed hourly scheduling of the system can also be performed to balance the daily supply and demand. Finally, the unutilized surplus energy can be used by incorporating a battery swapping system within the proposed charging station.

Nomenclature	
A	Area of wind turbine, m ²
$\dot{E}x_d$	Exergy destruction rate, kW
ex	Specific exergy, kJ/kg
h	Specific enthalpy, kJ/kg
\dot{m}	Mass flow rate, kg/s
P	Pressure, kPa
\dot{Q}	Heat rate, kW
s	Specific entropy, kJ/kg K
\dot{S}_{gen}	Entropy generation rate, kW/K
T	Temperature, K
V	Velocity, m/s
\dot{W}	Work rate, kW
Acronyms	
ACS	Absorption Cooling System
Comp.	Compound
CPV/T	Concentrated Photovoltaic–Thermal
EES	Engineering Equation Solver
EV	Electric Vehicle
FC	Fuel Cell
GHG	Greenhouse Gases
HTF	Heat Transfer Fluid
HVAC	Heating, Ventilation and Air Conditioning
MSW	Municipal Solid Wastes
PCM	Phase Change Material
PEV	Plug-in Electrical Vehicle
PV	Photovoltaic
RES	Renewable Energy Sources
TES	Thermal Energy Storage
Subscripts	
0	Reference state
CO ₂	Carbon Dioxide
en	energy
ex	exergy
H ₂	Hydrogen
H ₂ O	Water
LiBr	Lithium Bromide
Li-ion	Lithium Ion
N ₂	Nitrogen
NH ₃	Ammonia
NO _x	Nitrogen Oxides
Greek letters	
ϕ	Betz limit
ρ	Density of air
η	Efficiency

CRediT authorship contribution statement

Abdulla Al Wahedi: Formal analysis, Writing - original draft, Visualization, Investigation, Software, Validation. **Yusuf Bicer:** Conceptualization, Methodology, Software, Supervision, Writing - review & editing, Resources.

Declaration of competing interest

The authors declare that they have no known competing financial interests or personal relationships that could have appeared to influence the work reported in this paper.

Acknowledgment

The authors acknowledge the support provided by Hamad Bin Khalifa University, Qatar Foundation, Qatar (210009262). The publication of this article was funded by the Qatar National Library.

Appendix A. Supplementary data

Supplementary material related to this article can be found online at <https://doi.org/10.1016/j.egy.2020.07.022>.

References

- Al-nimr, M.A., Bukhari, M., Mansour, M., 2017. A combined CPV/T and ORC solar power generation system integrated with geothermal cooling and electrolyser / fuel cell storage unit. *Energy* 133, 513–524. <http://dx.doi.org/10.1016/j.energy.2017.05.142>.
- Al Wahedi, A., Bicer, Y., 2019. Assessment of a stand-alone hybrid solar and wind energy-based electric vehicle charging station with battery, hydrogen, and ammonia energy storages. *Energy Storage* 1. <http://dx.doi.org/10.1002/est2.84>.
- Al-Zareer, M., Dincer, I.R.M., 2018. A review of novel thermal management systems for batteries. *Int. J. Energy Res.* <http://dx.doi.org/10.1002/er.4095>.
- Al-zareer, M., Dincer, I., Rosen, M.A., 2018. A novel phase change based cooling system for prismatic lithium ion batteries Nouveau système de refroidissement à base de matériaux à changement de phase pour batteries lithium-ion prismatiques. *Int. J. Refrig.* 86, 203–217. <http://dx.doi.org/10.1016/j.ijrefrig.2017.12.005>.
- Al-zareer, M., Dincer, I., Rosen, M.A., 2019. A novel approach for performance improvement of liquid to vapor based battery cooling systems. <http://dx.doi.org/10.1016/j.enconman.2019.02.063>, 187, 191–204.
- Alves, P., Fernandes, J.F.P., Paulo, J., Torres, N., Branco, P.J.C., Fernandes, C., 2019. From Sweden to Portugal : the effect of very distinct climate zones on energy efficiency of a concentrating photovoltaic / thermal system (CPV/T). <http://dx.doi.org/10.1016/j.solener.2019.05.038>, 188, 96–110.
- Archer, S.A., Steinberger-wilckens, R., 2018. Sciencedirect systematic analysis of biomass derived fuels for fuel cells. *Int. J. Hydrogen Energy* 43, 23178–23192. <http://dx.doi.org/10.1016/j.ijhydene.2018.10.161>.
- Balat, H., Kirtay, E., 2010. Hydrogen from biomass e present scenario and future prospects. *Int. J. Hydrogen Energy* 35, 7416–7426. <http://dx.doi.org/10.1016/j.ijhydene.2010.04.137>.
- Bayram, I.S., Zamani, V., Hanna, R., Kleissl, J., 2016. On the evaluation of plug-in electric vehicle data of a campus charging network. In: 2016 IEEE Int Energy Conf ENERGYCON 2016. <http://dx.doi.org/10.1109/ENERGYCON.2016.7514026>.
- Bicer, Y., Dincer, I., 2015. Energy and exergy analyses of an integrated underground coal gasification with SOFC fuel cell system for multigeneration including hydrogen production. *Int. J. Hydrogen Energy* 40, 13323–13337. <http://dx.doi.org/10.1016/j.ijhydene.2015.08.023>.
- Biyik, E., Kahraman, A., 2019. A predictive control strategy for optimal management of peak load, thermal comfort, energy storage and renewables in multi-zone buildings. *J. Build Eng.* 25, 100826. <http://dx.doi.org/10.1016/j.jobbe.2019.100826>.
- Cadu, M., Huijbregts, M.A.J., Althaus, H., Koehler, A., Hellweg, S., 2012. Wind power electricity : The bigger the turbine, the greener the. <http://dx.doi.org/10.1021/es204108n>.
- Cui, T., Xuan, Y., Li, Q., 2016. Design of a novel concentrating photovoltaic-thermoelectric system incorporated with phase change materials. *Energy Convers. Manag.* 112, 49–60. <http://dx.doi.org/10.1016/j.enconman.2016.01.008>.
- Daneshazarian, R., Cuce, E., Cuce, P.M., Sher, F., 2018. Concentrating photovoltaic thermal (CPVT) collectors and systems: Theory, performance assessment and applications. *Renew. Sustain Energy Rev.* 81, 473–492. <http://dx.doi.org/10.1016/j.rser.2017.08.013>.
- EES, 2018. Chart, software engineering equations solver (EES).
- EWTDW 54 – 250 – 250, 00 kW - Wind turbine n.d., <https://en.wind-turbine-models.com/turbines/1538-ewtdw-54-250> (Accessed 8 May 2020).

- Ghasemi, A., Heidarnajad, P., Noorpoor, A., 2018. A novel solar-biomass based multi-generation energy system including water desalination and liquefaction of natural gas system: Thermodynamic and thermoeconomic optimization. *J. Clean Prod.* 196, 424–437. <http://dx.doi.org/10.1016/j.jclepro.2018.05.160>.
- Gholami, H., Sarwat, A.I., Hosseini, H., Khalilnejad, A., 2015. A evaluation of optimal dual axis concentrated photovoltaic thermal system with active ventilation using frog leap algorithm. *Energy Convers. Manag.* 105, 782–790. <http://dx.doi.org/10.1016/j.enconman.2015.08.033>.
- Girard, A., Roberts, C., Simon, F., Ordoñez, J., 2019. Solar electricity production and taxi electrical vehicle conversion in Chile. *J. Clean Prod.* 210, 1261–1269. <http://dx.doi.org/10.1016/j.jclepro.2018.11.092>.
- Inforlab Chemie, 2010. Determining the specific heat capacity of a battery pack. pp. 2–4.
- Khan, S.A., Bicer, Y., Koc, M., 2018. ScienceDirect Design and analysis of a multigeneration system with concentrating photovoltaic thermal (CPV/T) and hydrogen storage. <http://dx.doi.org/10.1016/j.ijhydene.2018.12.047>.
- Khan, N., Dilshad, S., Khalid, R., Kalair, A.R., Abas, N., 2019. Review of energy storage and transportation of energy. *Energy Storage* <http://dx.doi.org/10.1002/est2.49>, e49.
- Larminie, J., Dicks, A., 2013. Proton exchange membrane fuel cells. In: *Fuel Cell Syst. Explain.* John Wiley & Sons, Ltd, West Sussex, England, pp. 67–119. <http://dx.doi.org/10.1002/9781118878330.ch4>.
- Liu, L., Kong, F., Liu, X., Peng, Y., Wang, Q., 2015. A review on electric vehicles interacting with renewable energy in smart grid. *Renew. Sustain. Energy Rev.* 51, 648–661. <http://dx.doi.org/10.1016/j.rser.2015.06.036>.
- Mazzeo, D., 2019. Nocturnal electric vehicle charging interacting with a residential photovoltaic-battery system: a 3E (energy, economic and environmental) analysis. *Energy* 168, 310–331. <http://dx.doi.org/10.1016/j.energy.2018.11.057>.
- Mazzeo, D., Baglivo, C., Matera, N., Congedo, P.M., Oliveti, G., 2020. A novel energy-economic-environmental multi-criteria decision-making in the optimization of a hybrid renewable system. *Sustain. Cities Soc.* 52, 101780. <http://dx.doi.org/10.1016/j.scs.2019.101780>.
- Mehrjerdi, H., Hemmati, R., 2020. Energy and uncertainty management through domestic demand response in the residential building. *Energy* 192, 116647. <http://dx.doi.org/10.1016/j.energy.2019.116647>.
- Méndez, C., Bicer, Y., 2019. Wind energy potential of Qatar for power generation with associated financial and environmental benefits for natural gas industry. *Energies*.
- Mittal, M.L., 2010. Estimates of emissions from coal fired thermal power plants in India, 39 (2010) 1–22.
- Wind-turbine-models.com. EWT DW 54 – 250 – 250.00 kW - Wind turbine n.d. <https://en.wind-turbine-models.com/turbines/1538-ewt-dw-54-250> (Accessed 6 January 2020).
- Modi, A., Haglind, F., 2014. Performance analysis of a kalina cycle for a central receiver solar thermal power plant with direct steam generation. *Appl. Therm. Eng.* 65, 201–208. <http://dx.doi.org/10.1016/j.applthermaleng.2014.01.010>.
- Nixon, J.D., Dey, P.K., Davies, P.A., 2012. The feasibility of hybrid solar-biomass power plants in India. *Energy* 46, 541–554. <http://dx.doi.org/10.1016/j.energy.2012.07.058>.
- Notton, G., 2010. Hybrid Wind-Photovoltaic Energy Systems. Woodhead Publishing Limited, <http://dx.doi.org/10.1533/9781845699628.2.216>.
- Pesaran, A.A., 2002. Battery thermal models for hybrid vehicle simulations. 110, 377–382.
- Phase Change Material Products Limited, 2013. Plusice phase change materials phase. 3.
- Pro, O., 2017. CO2- Earth. Are We stabilising yet? Monthly CO2. Pro Oxygen. PVsyst 6.7.8 software, 2018.
- Qian, K., Zhou, C., Yuan, Y., Allan, M., 2010. Temperature effect on electric vehicle battery cycle life in vehicle-to-grid applications. In: 2010 China Int Conf Electr Distrib CIGRE 2010, 2010, pp. 1–6.
- Rabbani, M., Dincer, I., Naterer, G.F., 2012. Thermodynamic assessment of a wind turbine based combined cycle. *EGY 44*, 321–328. <http://dx.doi.org/10.1016/j.energy.2012.06.027>.
- REN21 Secretariat, 2015. Renewable global status report. Paris.
- REN21 Secretariat, 2016. Renewables global status report. Paris.
- Renno, C., 2014. Optimization of a concentrating photovoltaic thermal (CPV/T) system used for a domestic application. *Appl. Therm. Eng.* 67, 396–408. <http://dx.doi.org/10.1016/j.applthermaleng.2014.03.026>.
- Rodríguez-monroy, C., Mármol-acitores, G., Nilsson-cifuentes, G., 2018. Electricity generation in Chile using non-conventional renewable energy sources – a focus on biomass. *Renew. Sustain. Energy Rev.* 81, 937–945. <http://dx.doi.org/10.1016/j.rser.2017.08.059>.
- Sahoo, U., Kumar, R., Pant, P.C., Chaudhary, R., 2016. Resource assessment for hybrid solar-biomass power plant and its thermodynamic evaluation in India. *Sol. Energy* 139, 47–57. <http://dx.doi.org/10.1016/j.solener.2016.09.025>.
- Salem, M.R., Ali, R.K., Elshazly, K.M., 2017. Experimental investigation of the performance of a hybrid photovoltaic / thermal solar system using aluminium cooling plate with straight and helical channels. *Sol. Energy* 157, 147–156. <http://dx.doi.org/10.1016/j.solener.2017.08.019>.
- Suresh, N.S., Thirumalai, N.C., Dasappa, S., 2019. Modeling and analysis of solar thermal and biomass hybrid power plants. *Appl. Therm. Eng.* 160, 114121. <http://dx.doi.org/10.1016/j.applthermaleng.2019.114121>.
- The HOMER microgrid software Pro 2018 n.d.
- Usman Sajid, M., Bicer, Y., 2020. Thermodynamic assessment of chemical looping combustion and solar thermal methane cracking-based integrated system for green ammonia production. *Therm. Sci. Eng. Prog.* 19, 100588. <http://dx.doi.org/10.1016/j.tsep.2020.100588>.
- Wang, Z., Jochem, P., Fichtner, W., 2020. A scenario-based stochastic optimization model for charging scheduling of electric vehicles under uncertainties of vehicle availability and charging demand. *J. Clean Prod.* 254, 119886. <http://dx.doi.org/10.1016/j.jclepro.2019.119886>.
- Yang, F., Wang, H., Zhang, X., Tian, W., Hua, Y., Dong, T., 2018. Design and experimental study of a cost-effective low concentrating photovoltaic / thermal system. *Sol Energy* 160, 289–296. <http://dx.doi.org/10.1016/j.solener.2017.12.009>.
- Zou, Y., Zhao, J., Gao, X., Chen, Y., Tohidi, A., 2020. Experimental results of electric vehicles effects on low voltage grids. *J. Clean Prod.* 255, 120270. <http://dx.doi.org/10.1016/j.jclepro.2020.120270>.